

A novel approach for preparing silver nanoparticles under electron beam irradiation

Kai Li · Fu-Shen Zhang

Received: 15 October 2008 / Accepted: 23 June 2009 / Published online: 12 July 2009
© Springer Science+Business Media B.V. 2009

Abstract Silver (Ag) nanoparticles were obtained when Ag microparticles were exposed to an electron beam in a transmission electron microscope (TEM). Results from TEM characterization indicated that the morphologies of the prepared Ag nanoparticles were quasi-circular, and the sizes were mainly in the range of 5–60 nm. The effect of irradiation time (t) on size and distribution of Ag nanoparticles was investigated. It was found that the sizes of Ag nanoparticles increased with the increase of t . The bigger Ag nanoparticles were near the Ag microparticle and the smaller ones were far from it. In addition, these Ag nanoparticles were monodisperse. This approach offered a new route for preparing Ag nanoparticles under electron beam irradiation, and the forming process of Ag nanoparticles was explained by the nucleation-growth mechanism.

Keywords Ag nanoparticles · Ag microparticles · Electron beam irradiation method · Calcination method · Irradiation time · Nucleation-growth mechanism · Synthesis

Introduction

Silver (Ag) nanoparticles are widely used in microelectronics, photoelectron materials, electronic conduction materials, and catalyst, etc., due to their unique electrical, magnetic, and other properties (Kukhta et al. 2006; Ma et al. 2008; Liu and Zhao 2009). In the field of spectroscopy, Ag nanoparticles show good surface-enhanced Raman scattering (SERS) effects (Nie and Emory 1997; Wang et al. 2006). In addition, Ag nanoparticles have antibacterial capability (Baker et al. 2005; Shrivastava et al. 2007; Martinez-Castanon et al. 2008). When Ag nanoparticles are added into some fibers, the characteristics of these fibers are improved, and simultaneously the fibers also have antibacterial capability. As Ag nanoparticles have these merits as above mentioned, many methods were used for Ag nanoparticle preparation, including electrochemical deposition (Rodriguez-Sanchez et al. 2000; Khaydarov et al. 2008), polymer-protected reduction (Zhang et al. 1996; Yonezawa et al. 2001), microemulsion (Ji et al. 1999; Shah et al. 2000), and hydrothermal methods (Wang et al. 2005).

In recent years, electron beam irradiation method has been widely used to prepare metal nanoparticles. For example, highly monodisperse gold nanoparticles with an average diameter of 2.0 nm were obtained when the Au(I)-SC₁₈ polymer was irradiated by an electron beam in a TEM (Kim et al. 2005). Bismuth nanoparticles were synthesized when sodium

K. Li · F.-S. Zhang (✉)
Research Center for Eco-Environmental Sciences,
Chinese Academy of Sciences, Beijing,
People's Republic of China
e-mail: fszhang@rcees.ac.cn

bismuthate was exposed to an electron beam in a TEM (Sepulveda-Guzman et al. 2007). After the electron beam irradiation, bismuth nanoparticles with a rhombohedral structure and diameter of 6 nm were observed. To our best knowledge, however, there are no reported studies of using Ag microparticles as precursors to prepare Ag nanoparticles by electron beam irradiation method. In this article, Ag microparticles were first prepared by calcination method, and then Ag nanoparticles were obtained using these Ag microparticles under electron beam irradiation in a TEM. As a result, a new approach for preparing Ag nanoparticles was established.

Experimental section

The experimental process was as follows: First, 1.0 g of silver chloride (AgCl) and 2.0 g of sodium carbonate (Na_2CO_3 , keeping in excess) were mixed homogeneously in a ceramic crucible. Then the ceramic crucible was placed in muffle and heated at 500 °C for 3 h. Second, the muffle was cooled down to room temperature, and the product was filtered and washed with distilled water to remove the by-products. The product was then dried at 80 °C under vacuum for 2–3 h. Finally, the prepared sample was sonicated in methanol for 30 min before 2–3 drops of the suspension were transformed onto a 3-mm diameter holey carbon-coated copper grid. The solvent was allowed to evaporate at room temperature before loading the sample in a Hitachi H-7500 TEM. Then, with an accelerating voltage of 80 kV and a beam current of 12 μA , the sample was irradiated by an electron beam.

The phase of the sample was identified by X-ray diffraction (XRD) patterns, which was taken on a Philip X'pert X-ray diffractometer (Cu K_{α} , $V = 40$ kV, $I = 40$ mA). Prior to the measurement, the sample was ground thoroughly in an agate mortar.

Results and discussion

XRD pattern of the sample is shown in Fig. 1. As demonstrated in Fig. 1, there exist four diffraction peaks located at $2\theta = 38.1^\circ$, 44.3° , 64.5° , and 77.4° , respectively. Compared with data from Powder Diffraction File No. 04-0783, these peaks can be assigned to the (111), (200), (220), and (311) planes

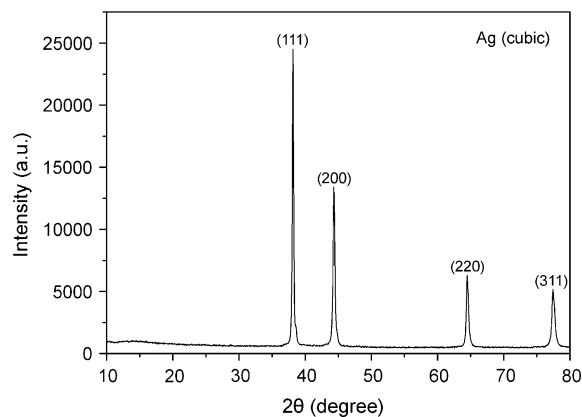


Fig. 1 XRD pattern of Ag particles prepared by calcination method

of face-centered cubic (fcc) phase of Ag (He et al. 2007). This result means that cubic Ag was prepared by calcination method.

TEM was used to observe the morphologies of the samples. TEM images of the sample prepared by calcination method are shown in Fig. 2. In Fig. 2a, b, there are many particles. These particles are quasi-circular and the average size of them is approximately 2 μm . Moreover, most of these microparticles aggregate together. Combined with XRD result, it is believed that the component of these microparticles is Ag. These microparticles are all Ag microparticles.

In Fig. 3a, there is a big quasi-circular Ag microparticle in the center. The size of the big quasi-circular particle is about 5 μm . This big Ag microparticle was formed by melting some small Ag microparticles under electron beam irradiation. When the electron beam focused on some small Ag microparticles (shown in Fig. 2), these small Ag microparticles melted and merged with each other to form a big Ag microparticle. In particular, irradiation heated the small Ag microparticle by energy absorption. As a result, the big Ag microparticle was formed under electron beam irradiation. The forming process was so quick that TEM images of this process could not be obtained.

With the increase of irradiation time (t , approximately 5 s after the electron beam focused on the big Ag microparticle), the big Ag microparticle (shown in Fig. 3a), formed by melting small Ag microparticles, obtained excess energy. Then, it was bombarded by the electron beam to produce a smaller Ag microparticle and lots of Ag nanoparticles (shown in

Fig. 2 TEM images of Ag microparticles prepared by calcination method

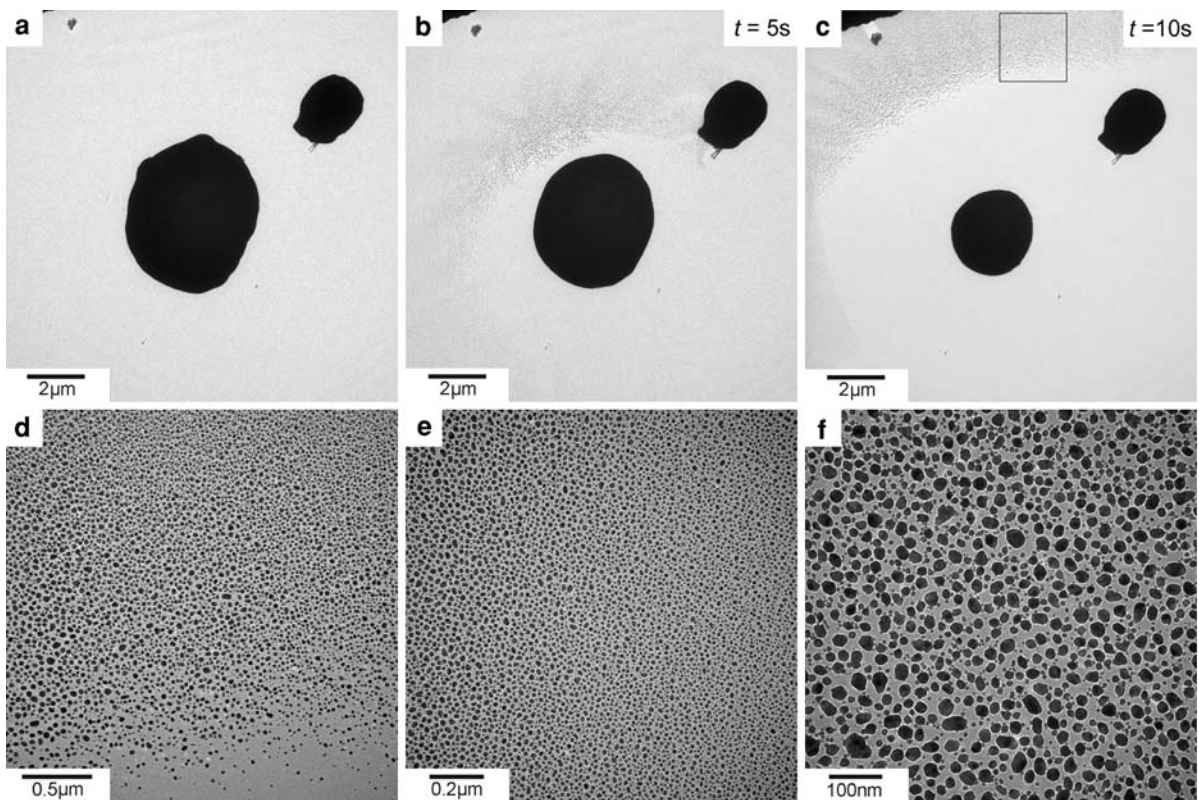
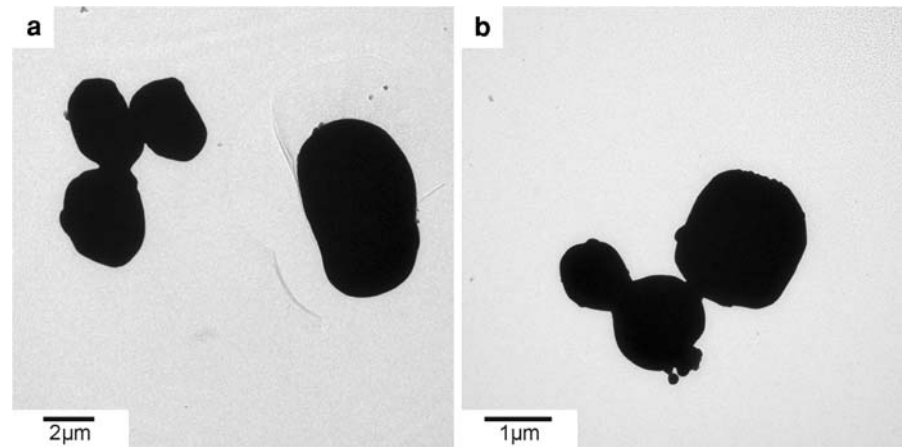


Fig. 3 The bombardment process under TEM and TEM images of Ag nanoparticles

Fig. 3b). If t is increased further (approximately 10 s), then the size of the big Ag microparticle decreased further (about $3 \mu\text{m}$ in the center of Fig. 3c). On the contrary, the number of the Ag nanoparticles (on the top of Fig. 3c) increased dramatically. Fortunately, the bombardment process was observed under TEM (see Fig. 3a–c).

Figure 3d is a magnified image obtained from the marked area of the Ag nanoparticles in Fig. 3c. Higher magnification images of Fig. 3d are shown in Fig. 3e, f. Parts d–f of Fig. 3 illustrate the morphologies of the prepared Ag nanoparticles. On an analysis of the Fig. 3f, it can be seen that the morphologies of these Ag nanoparticles are quasi-

circular, and their sizes are mainly in the range of 5–60 nm. In addition, these Ag nanoparticles are monodisperse.

In order to investigate the effect of t on size and distribution of Ag nanoparticles, t was increased from 10 s to 20 s while the accelerating voltage (V) was kept at 80 kV. Ag microparticle with the diameter of about 3 μm is found in the center of Fig. 4a (approximately 10 s after the electron beam was focused on the big Ag microparticle). A lot of Ag nanoparticles are found around it. Figure 4b is a magnified image obtained from the marked area in Fig. 4a. Similar to Fig. 3d, an analysis of Fig. 4b reveals that the morphologies of these Ag nanoparticles are quasi-circular, and their sizes are mainly in the range of 5–60 nm. Moreover, these Ag nanoparticles are also monodisperse.

In Fig. 4c, with the increase of t (approximately 20 s), the size of the Ag microparticle decreased further (about 2 μm in the center of Fig. 4c). However, the number of the Ag nanoparticles increased dramatically. A magnified image obtained from the marked area in Fig. 4c and shown in Fig. 4d reveals that the morphologies of Ag nanoparticles are still quasi-circular in shape and monodisperse. In contrast with Fig. 4b, the sizes of Ag nanoparticles have increased, which are mainly in the range of 10–90 nm. Furthermore, the bigger Ag nanoparticles are near the Ag microparticle. The smaller ones are distributed in the outer region of Fig. 4c, far from the Ag microparticle.

The forming process of Ag nanoparticles can be explained by the nucleation-growth mechanism as follows:

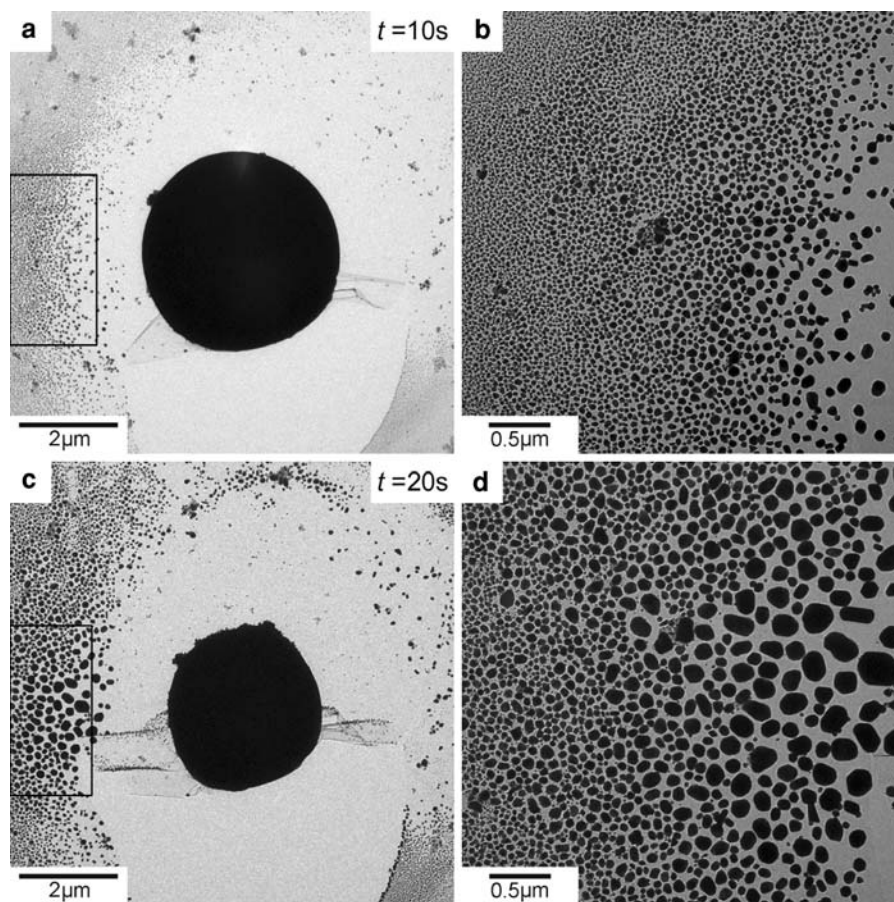
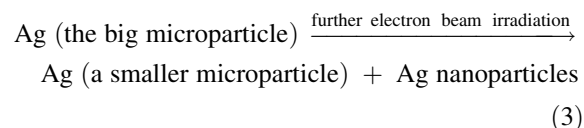
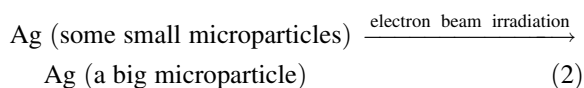
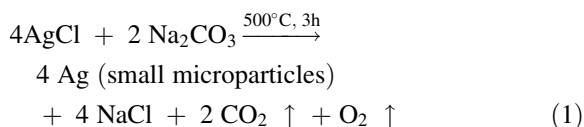


Fig. 4 TEM images of Ag nanoparticles prepared at different t



In this study, Ag microparticles (shown in Fig. 2) were first prepared by calcination method (step 1). When the electron beam was focused on small Ag microparticles, these small Ag microparticles melted and merged with each other to form a big Ag microparticle (shown in Fig. 3a) (step 2). With the increase of t (approximately 10 s), the big Ag microparticle obtained excess heat energy and was bombarded to produce a smaller Ag microparticle due to the continuous irradiation of the focused electron beam. Simultaneously, the “missing” part of Ag microparticle (Ag droplets) would be sputtered around the Ag microparticle (shown in Figs. 3c, 4a). As the sputtering process was rapid and the temperature of the “missing” part of Ag microparticle decreased quickly, the high degree of supersaturation formed within a very short time, thus giving rise to the high nucleation rates of Ag. As a result, these Ag nuclei grew rapidly, and a lot of Ag nanoparticles (5–60 nm, shown in Figs. 3c, 4a) were obtained (step 3). This procedure could be explained in terms of the processes of nucleation and subsequent growth of Ag nanoparticles (Ahn et al. 2006; Manuel et al. 2007).

If t is increased further (approximately 20 s), the “missing” part of Ag microparticle would continue to be sputtered around the Ag microparticle (shown in Fig. 4c). At this moment, many Ag nanoparticles (5–60 nm, shown in Fig. 4b) would grow continuously into bigger Ag nanoparticles leading to the sputtering of the “missing” part of Ag microparticle. Thus, the sizes of Ag nanoparticles increased, mainly in the range of 10–90 nm (shown in Fig. 4d). On the other hand, Ag nanoparticles near the Ag microparticle would restrain the sputtering of the “missing” part of Ag microparticle toward the outer region. As a result, the sizes of Ag nanoparticles near the Ag microparticle were bigger than the sizes of those far from it (shown in Fig. 4c).

Conclusions

Ag nanoparticles (quasi-circular, 5–60 nm, and monodisperse) can be obtained from Ag microparticles under electron beam irradiation. The effect of t on size and distribution of Ag nanoparticles was discussed. It was found that, with the increase of t (approximately 20 s), Ag nanoparticles were still in quasi-circular shape and monodisperse. However, the sizes of Ag nanoparticles increased (10–90 nm). In addition, the bigger Ag nanoparticles were near the Ag microparticle and the smaller ones were far from it due to the restrained-sputtering effect. The effects of V and beam current on size and distribution of Ag nanoparticles also will be investigated in the future. It is believed that, monodisperse Ag nanoparticles with smaller size can be obtained using this approach by optimizing these parameters. Further experimental study to separate Ag nanoparticles from Ag microparticles in the presence of surfactant by centrifugal separation method and to apply these Ag nanoparticles as catalyst for the selective oxidation of styrene and the reduction of aromatic nitrocompounds also needs to be carried out.

Acknowledgments This research was financially supported, in part, by the National Key Technology R&D Program (2008BAC32B03) and the National Basic Research Program (2007CB407303) of China. The authors thank Prof. Zheng-Ping Hao for his helpful discussion and improving upon this manuscript.

References

- Ahn SJ, Kim KH, Chun YG et al (2006) Nucleation and growth of Cu(In, Ga)Se₂ nanoparticles in low temperature colloidal process. *Thin Solid Films* 515:4036–4040. doi: [10.1016/j.tsf.2006.10.102](https://doi.org/10.1016/j.tsf.2006.10.102)
- Baker C, Pradhan A, Pakstis L et al (2005) Synthesis and antibacterial properties of silver nanoparticles. *J Nanosci Nanotechnol* 5:244–249. doi: [10.1166/jnn.2005.034](https://doi.org/10.1166/jnn.2005.034)
- He X, Zhao XJ, Chen YX et al (2007) Synthesis and characterization of silver nanowires with zigzag morphology in N,N-dimethylformamide. *J Solid State Chem* 180:2262–2267. doi: [10.1016/j.jssc.2007.05.023](https://doi.org/10.1016/j.jssc.2007.05.023)
- Ji M, Chen XY, Wai CM et al (1999) Synthesizing and dispersing silver nanoparticles in a water-in-supercritical carbon dioxide microemulsion. *J Am Chem Soc* 121:2631–2632. doi: [10.1021/ja9840403](https://doi.org/10.1021/ja9840403)
- Khaydarov RA, Khaydarov RR, Gapurova O et al (2008) Electrochemical method for the synthesis of silver nanoparticles. *J Nanopart Res* doi: [10.1007/s11051-008-9513-x](https://doi.org/10.1007/s11051-008-9513-x)

- Kim JU, Cha SH, Shin K et al (2005) Synthesis of gold nanoparticles from gold(I)-alkanethiolate complexes with supramolecular structures through electron beam irradiation in TEM. *J Am Chem Soc* 127:9962–9963. doi:[10.1021/ja042423x](https://doi.org/10.1021/ja042423x)
- Kukhta AV, Kolesnik EE, Lesnikovich AI et al (2006) Optical and electrophysical properties of Ag-PEPC nanocomposites. *Mater Sci Eng C* 26:1012–1016. doi:[10.1016/j.msec.2005.09.041](https://doi.org/10.1016/j.msec.2005.09.041)
- Liu P, Zhao MF (2009) Silver nanoparticle supported on halloysite nanotubes catalyzed reduction of 4-nitrophenol (4-NP). *Appl Surf Sci* 255:3989–3993. doi:[10.1016/j.apsusc.2008.10.094](https://doi.org/10.1016/j.apsusc.2008.10.094)
- Ma PC, Tang BZ, Kim JK (2008) Effect of CNT decoration with silver nanoparticles on electrical conductivity of CNT-polymer composites. *Carbon* 46:1497–1505. doi:[10.1016/j.carbon.2008.06.048](https://doi.org/10.1016/j.carbon.2008.06.048)
- Manuel AM, Catarina S, Maria MA et al (2007) Hydroxyapatite micro- and nanoparticles: nucleation and growth mechanisms in the presence of citrate species. *J Colloid Interface Sci* 318:210–216. doi:[10.1016/j.jcis.2007.10.008](https://doi.org/10.1016/j.jcis.2007.10.008)
- Martinez-Castanon GA, Nino-Martinez N, Martinez-Gutierrez F et al (2008) Synthesis and antibacterial activity of silver nanoparticles with different sizes. *J Nanopart Res* 10:1343–1348. doi:[10.1007/s11051-008-9428-6](https://doi.org/10.1007/s11051-008-9428-6)
- Nie SM, Emory SR (1997) Probing single molecules and single nanoparticles by surface-enhanced Raman scattering. *Science* 275:1102–1106. doi:[10.1126/science.275.5303.1102](https://doi.org/10.1126/science.275.5303.1102)
- Rodriguez-Sanchez L, Blanco MC, Lopez-Quintela MA (2000) Electrochemical synthesis of silver nanoparticles. *J Phys Chem B* 104:9683–9688. doi:[10.1021/jp001761r](https://doi.org/10.1021/jp001761r)
- Sepulveda-Guzman S, Elizondo-Villarreal N, Ferrer D et al (2007) In situ formation of bismuth nanoparticles through electron-beam irradiation in a transmission electron microscope. *Nanotechnology* 18:335604–335609. doi:[10.1088/0957-4484/18/33/335604](https://doi.org/10.1088/0957-4484/18/33/335604)
- Shah PS, Holmes JD, Doty RC et al (2000) Steric stabilization of nanocrystals in supercritical CO₂ using fluorinated ligands. *J Am Chem Soc* 122:4245–4246. doi:[10.1021/ja9943748](https://doi.org/10.1021/ja9943748)
- Shrivastava S, Bera T, Roy A et al (2007) Characterization of enhanced antibacterial effects of novel silver nanoparticles. *Nanotechnology* 18:225103–225111. doi:[10.1088/0957-4484/18/22/225103](https://doi.org/10.1088/0957-4484/18/22/225103)
- Wang X, Zhuang J, Peng Q et al (2005) A general strategy for nanocrystal synthesis. *Nature* 437:121–124. doi:[10.1038/nature03968](https://doi.org/10.1038/nature03968)
- Wang HH, Liu CY, Wu SB et al (2006) Highly Raman-enhancing substrates based on silver nanoparticle arrays with tunable sub-10 nm gaps. *Adv Mater* 18:491–495. doi:[10.1002/adma.200501875](https://doi.org/10.1002/adma.200501875)
- Yonezawa T, Onoue S, Kimizuka N (2001) Self-organized superstructures of fluorocarbon-stabilized silver nanoparticles. *Adv Mater* 13:140–142. doi:[10.1002/1521-4095\(200101\)13:2<140::AID-ADMA140>3.0.CO;2-H](https://doi.org/10.1002/1521-4095(200101)13:2<140::AID-ADMA140>3.0.CO;2-H)
- Zhang ZT, Zhao B, Hu LM (1996) PVP protective mechanism of ultrafine silver powder synthesized by chemical reduction processes. *J Solid State Chem* 121:105–110. doi:[10.1006/jssc.1996.0015](https://doi.org/10.1006/jssc.1996.0015)